

PL3: Structure Functions* OUNP-98-01

Robin Devenish (r.devenish@physics.ox.ac.uk)

Physics Dept., Oxford University, UK

Abstract. Recent measurements of unpolarised and polarised nucleon structure functions and F_2^γ are reviewed. The implications for QCD and the gluon momentum distribution are discussed. The status of the understanding of $\sigma_{tot}^{\gamma^*p}$ in the transition region between real photoproduction and deep-inelastic scattering is summarised briefly.

1 Introduction

This talk covers three areas: unpolarised deep-inelastic scattering (DIS) data, parton distributions and associated phenomenology (Sec. 2); nucleon spin structure (Sec. 3) and the status of F_2^γ measurements (Sec. 4). New measurements from the Tevatron relevant for parton determination such as W decay asymmetries, Drell-Yan asymmetries, direct γ and inclusive jet cross-sections are covered by Weerts [1]. Diffractive DIS and the diffractive structure function are covered by Eichler [2], recent measurements of α_S by Ward [3] and the status of DIS measurements at very large Q^2 from HERA are summarised by Elsen [4].

2 Unpolarised Deep Inelastic Scattering

The kinematic variables describing DIS are $Q^2 = -(k - k')^2$, $x = Q^2/(2p \cdot q)$, $y = (p \cdot q)/(p \cdot k)$, where $q = k - k'$ and k, k', p are the 4-momenta of the initial and final lepton and target nucleon respectively. At fixed s , where $s = (k + p)^2$, and ignoring masses the variables are related by $Q^2 = sxy$. The expression for the double differential neutral-current DIS cross-section is

$$\frac{d^2\sigma(l^\pm N)}{dx dQ^2} = \frac{2\pi\alpha^2}{Q^4 x} [Y_+ F_2(x, Q^2) - y^2 F_L(x, Q^2) \mp Y_- xF_3(x, Q^2)], \quad (1)$$

where $Y_\pm = 1 \pm (1 - y)^2$ and F_i ($i = 2, 3, L$) are the nucleon structure functions. For Q^2 values much below that of the Z^0 mass squared, the parity violating structure function xF_3 is negligible. F_L is a significant contribution only at large y . At HERA both F_3 and F_L are treated as calculated corrections and the F_2 data quoted is that corresponding to γ^* exchange only. The kinematic coverage of recent fixed target and HERA collider experiments is shown in Fig. 1 and more details are given in Table 1.

* Extended version of the writeup of the plenary talk given at the EPS HEP97 Conference, Jerusalem Aug. 1997.

Table 1. Summary of recent structure function experiments. All the data referred in this table are available from the Durham HEPDATA database, at <http://durpdg.dur.ac.uk/HEPDATA> on the world wide web.

Beam(s)	Targets	Experiment	Q^2 (GeV^2)	x	R	Status
e^-	p,d,A	SLAC	0.6 – 30	0.06 – 0.9	yes	complete
μ	p,d,A	BCDMS	7 – 260	0.06 – 0.8	yes	complete
μ	p,d,A	NMC	0.5 – 75	0.0045 – 0.6	yes	complete
μ	p,d,A	E665	0.2 – 75	$8 \cdot 10^{-4}$ – 0.6	no	complete
$\nu, \bar{\nu}$	Fe	CCFR	1. – 500.	0.015 – 0.65	yes	complete
e^\pm, p	-	H1	0.35 – 5000	$6 \cdot 10^{-6}$ – 0.32	estimate	running
e^\pm, p	-	ZEUS	0.16 – 5000	$3 \cdot 10^{-6}$ – 0.5	no	running

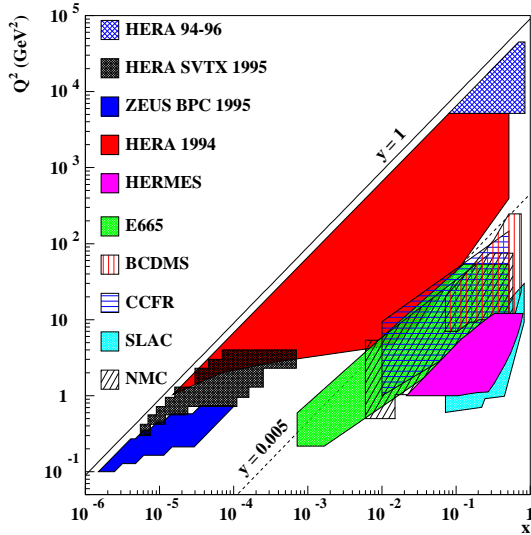


Fig. 1. Regions in the (x, Q^2) plane for fixed target and collider DIS experiments.

The vast bulk of nucleon structure function data is for F_2 and here the overall situation is rather pleasing. The fixed target programme is complete with the publication in the last 18 months of the final data from NMC [5] and E665 [6] to add to the older data from SLAC and BCDMS that still play an important role in global fits to determine parton distribution functions (PDFs). The first high statistics data from the 1994 HERA run were pub-

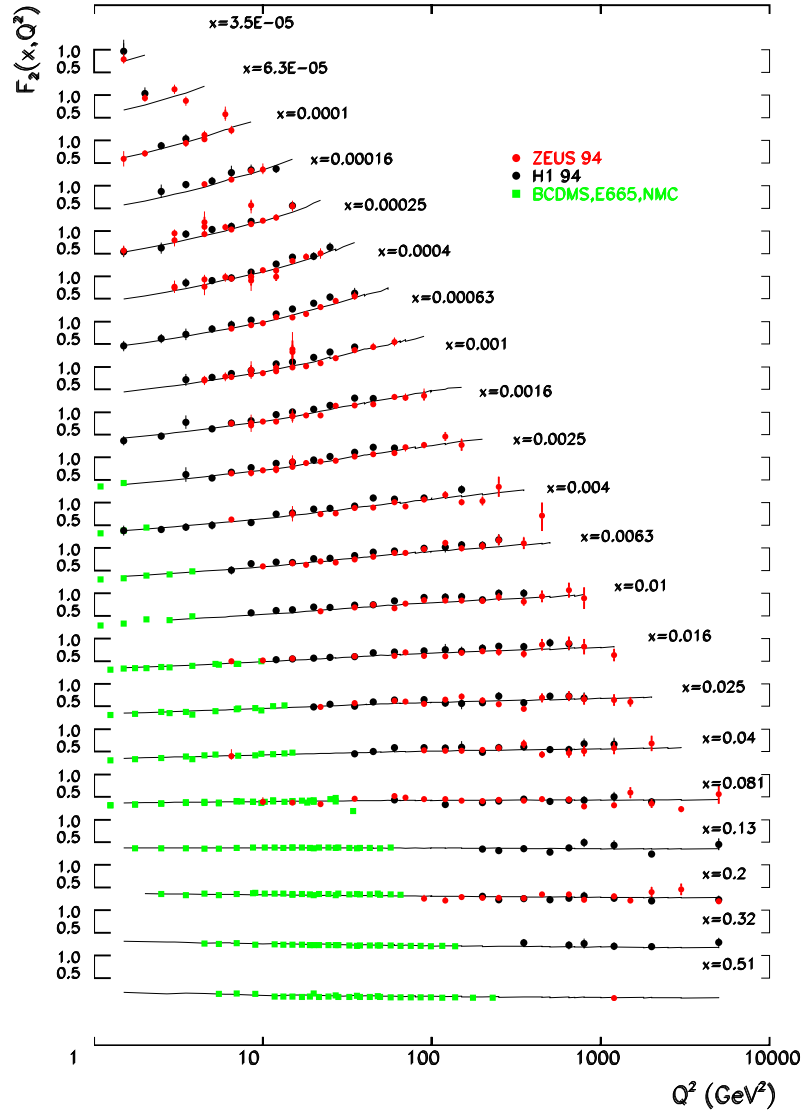


Fig. 2. F_2^p data from HERA(94) and fixed target experiments at fixed x as a function of Q^2 . The curves shown are the NLO DGLAP QCD fit used to smooth the data during unfolding.

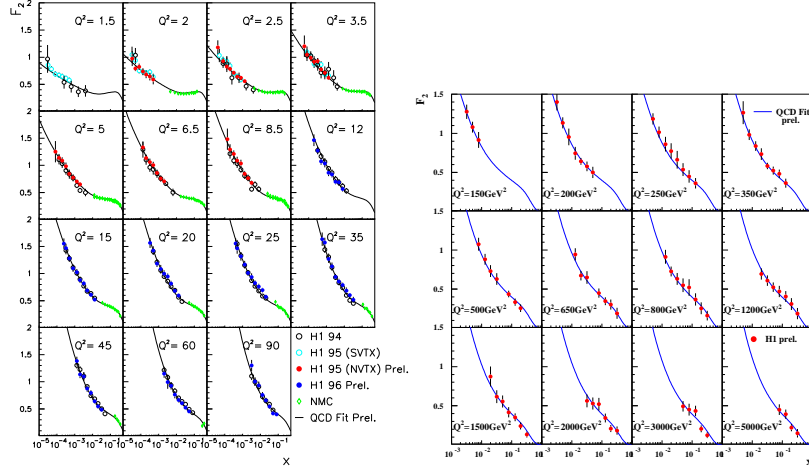


Fig. 3. Preliminary H1 F_2 data: left $1 < Q^2 < 100 \text{ GeV}^2$ from HERA 1995/6; right $150 < Q^2 < 5000 \text{ GeV}^2$ from HERA 1995-97 runs. The curves show the Q^2 evolution of a NLO QCD fit to H1 data on the left and evolved to higher Q^2 .

lished by H1 [7] and ZEUS [8] last year. The F_2 data now covering 4 decades in Q^2 and 5 decades in x are summarised in Fig. 2. The data from the fixed target and HERA collider experiments are consistent with each other in shape and normalisation and show the pattern of scaling violations expected from perturbative QCD (pQCD). The systematic errors for the fixed target experiments are typically less than 5% and those for H1 and ZEUS around 5% for $Q^2 < 100 \text{ GeV}^2$, above this value the errors become statistics dominated. Fairly recently CCFR published an update of their high statistics $F_2^{\nu Fe}$ and $x F_3^{\nu Fe}$ data [9], following an improved determination of energy calibrations. The CCFR data and a determination of α_S are described in more detail by De Barbaro [10].

H1 has submitted preliminary values of F_2 from more recent HERA runs. The data are shown in Fig. 3: on the left for $1 < Q^2 < 100 \text{ GeV}^2$ (the region covered by the improved H1 rear detector) is from 5.4 pb^{-1} taken in 1995/96 [11]; on the right for $150 < Q^2 < 5000 \text{ GeV}^2$ is from 22 pb^{-1} accumulated over the period 1995-97 [12]. Also shown in Fig. 3 is a NLO QCD fit to H1 data with $Q^2 < 120 \text{ GeV}^2$, which is evolved to cover the region of the higher Q^2 data. All the new data are well described by the QCD curves and the characteristic step rise of F_2 as x decreases is seen up to the largest Q^2 values.

2.1 The low Q^2 transition region

One of the surprises of the HERA F_2 data is the low scale from which NLO QCD evolution seems to work. H1 and ZEUS have now measured the cross-sections and hence F_2 from the safely DIS at $Q^2 \sim 6 \text{ GeV}^2$ through the transition region to $Q^2 = 0$, using a combination of new detectors very close to the electron beam line and by shifting the primary interaction vertex in the proton direction by 70 cm. The data are shown in Fig. 4 and are described in detail in refs. [13, 14, 15]. Also shown in the figure are data from the E665 experiment [6] which had a special trigger to allow measurements at small x and Q^2 . As $Q^2 \rightarrow 0$ F_2 must tend to zero at least as fast as Q^2 , it is often more convenient to consider

$$\sigma_{tot}^{\gamma^*p}(W^2, Q^2) \approx \frac{4\pi^2\alpha}{Q^2} F_2(x, Q^2) \quad (2)$$

which is valid for small x and where $W^2 \approx Q^2/x$ is the centre-of-mass energy squared of the γ^*p system. For $Q^2 > 1 \text{ GeV}^2$, the steep rise of F_2 as x decreases is reflected in a steeper rise of $\sigma_{tot}^{\gamma^*p}$ with W^2 than the slow increase shown by $\sigma_{tot}^{\gamma p}$ and characteristic of hadron-hadron total cross-sections.

Two very different approaches, both proposed before the HERA measurements, may be taken as paradigms. Glück, Reya and Vogt (GRV) [16] have long advocated a very low starting scale as part of their approach to generate PDFs ‘dynamically’ using NLO QCD. Predictions from their most recent parameterisation [17] are shown as the black solid line in Fig. 4, starting in the $Q^2 = 0.4 \text{ GeV}^2$ bin and upwards. The data are in reasonable agreement with the theory down as far as the $Q^2 = 0.92 \text{ GeV}^2$ bin. The other approach, that of Donnachie and Landshoff (DL) [18], is an extension of Regge parameterisations that describe hadron-hadron and real photoproduction data well. The form that DL use to describe $\sigma_{tot}^{\gamma^*p}$ is

$$\sigma_{DL} = A(Q^2)(W^2)^{\alpha_P-1} + B(Q^2)(W^2)^{\alpha_R-1}, \quad (3)$$

where α_P and α_R are the intercepts of the Pomeron and Reggeon trajectories respectively with values $\alpha_P = 1.08$, $\alpha_R = 0.05$, determined from hadron-hadron data. The DL model gives the trend of the energy dependence of the very low Q^2 $\sigma_{tot}^{\gamma^*p}$ HERA data, up to $Q^2 \sim 0.4 \text{ GeV}^2$, though the normalisation of the model is a bit on the low side. The DL curves in Fig. 4 are the solid grey lines. In [19] the ZEUS collaboration has investigated the transition region. From NLO QCD fits with starting scales of $Q_0^2 = 0.4, 0.8, 1.2 \text{ GeV}^2$ it is found that only the latter two give acceptable descriptions of the data. For the limit $Q^2 \rightarrow 0$ a DL form is used. From these two approaches the transition to pQCD occurs in the Q^2 range $0.8 - 1.2 \text{ GeV}^2$.

The advent of accurate data from HERA has prompted many groups to try to model the behaviour of $\sigma_{tot}^{\gamma^*p}$ throughout the transition region. Very briefly: the model of Capella et al (CKMT) [20] uses a DL form at

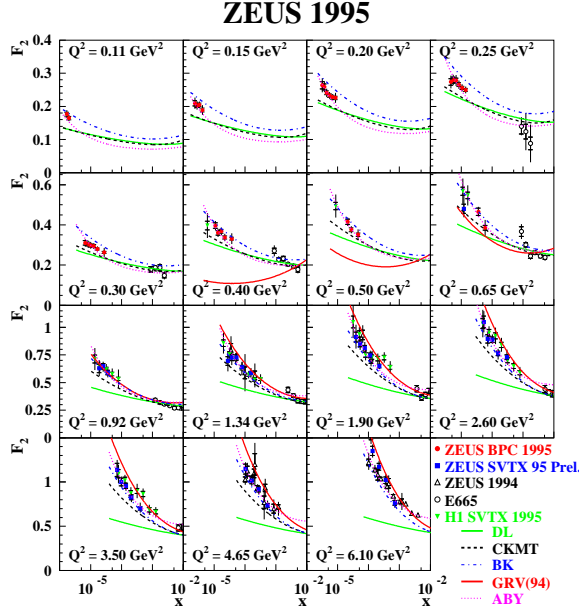


Fig. 4. F_2 data from E665, H1 and ZEUS at very small values of Q^2 . The curves are described in the text.

low Q^2 but allows the Regge intercepts α_P , α_R to become Q^2 dependent, for $Q^2 > 2 \text{ GeV}^2$ DGLAP evolution gives the Q^2 dependence; Abramowicz et al (ALLM) [21] follow a similar approach but use a QCD inspired parameterisation at large Q^2 ; Badelek & Kwiecinski (BK) [22] take $F_2 = F_2^{VMD} + Q^2 F_2^{QCD} / (Q^2 + Q_0^2)$ where F_2^{VMD} is given by strict ρ , ω , ϕ VMD and the QCD scale parameter Q_0^2 is chosen to be 1.2 GeV^2 ; Schildknecht and Spiesberger (ScSp) [23] revive the idea of GVMD to fit data for $0 < x < 0.05$ and $0 < Q^2 < 350 \text{ GeV}^2$; Kerley and Shaw [24] modify the idea of long-lived hadronic fluctuations of the photon to include jet production; Gotsman, Levin & Maor [25] also follow this approach but have an additional hard QCD term; finally Adel, Barreiro & Yndurain (ABY) [26] have developed a model with an input x dependence of the form $a + bx^{-\lambda}$ with the two terms representing ‘soft’ and ‘hard’ contributions which evolve independently with Q^2 . Fig. 4 shows some of these models against the low Q^2 data. Although most of them give a reasonable description of the trends in x and Q^2 , only the ScSp and ABY models (which were fit to the data) give the details correctly. In fact these two models also have defects as they are not able to describe the low

energy $\sigma_{tot}^{\gamma p}$ data [27]. Very recently Abramowicz and Levy [28] have updated the ALLM parameterisation by including all the recent HERA data in the fit and result gives a satisfactory description of both the Q^2 and W^2 dependence. However, while this represents an advance, it is still true to say that more work needs to be done before the low Q^2 , low x region is completely understood. More details of many of these models are given in the review by Badelek and Kwiecinski [29].

2.2 QCD and parton distributions

The striking rise of F_2 as x decreases was at first thought, at least by some, to be evidence for the singular behaviour of the gluon density $xg \sim x^{-\lambda}$ with $\lambda \sim 0.3 - 0.5$ proposed by Balitsky et al [30] (BFKL) and a breakdown of ‘conventional’ pQCD as embodied in the DGLAP equations. By the time of the EPS HEP95 conference in Brussels [31] the pendulum had swung the other way, largely through the work of Ball & Forte [32] on ‘double asymptotic scaling’ (DAS) and the success of GRV(94) [17] in describing the data. In both cases the rise in F_2 is generated through the DGLAP kernels with a non-singular input. It is clear from Figs. 2, 3 that NLO DGLAP Q^2 evolution can describe the F_2 data from $Q^2 \approx 1.5 \text{ GeV}^2$ to the highest values of 5000 GeV^2 . The two global fitting teams in their most recent determinations of the PDFs (CTEQ4 [33] and MRS(R) [34]), which include the HERA 1994 data, now use starting scales of around 1 GeV^2 . The quality of the fits is good with χ^2/ndf in the range $1.06 - 1.33$ and it is found that the gluon distribution is now non-singular in x at the input scale with the quark sea still mildly singular. Both CTEQ and MRS give PDFs for $\alpha_S(M_Z^2)$ in the range $0.113 - 0.120$ as there is some indication that the more recent determinations [3, 35] give a somewhat larger value than the ‘DIS value’ of 0.113 determined from a fit to BCDMS and SLAC data [36]. The extension of accurate measurements to low x provided by the HERA(94) data has led to a big improvement in the knowledge of the gluon density. At low x the gluon drives the scaling violations through $\frac{dF_2}{d \ln Q^2} \sim \alpha_S P_{gg} g(x, Q^2)$. Apart from the global fits already mentioned both ZEUS and H1 have performed NLO QCD fits to extract $xg(x, Q^2)$. The advantage that the experimental teams have is that they can include a full treatment of systematic errors. Since HERA data does not extend to large x fixed target DIS data has to be included to fix the parameters of the valence quark distributions. ZEUS uses its 1994 HERA data and a fixed $\alpha_S = 0.113$, H1 fits HERA 1995/96 data and $\alpha_S = 0.118$ More details are given by Priniias [37]. The resulting gluon distributions are shown in Fig. 5(left) together with that from the NMC experiment and some curves from global fits. The total error is about 10% at the lowest x values. All determinations agree within the error bands except for GRV(94) which was not fit to the HERA(94) data and which does not describe the recent HERA data in detail. Part of the discrepancy comes from

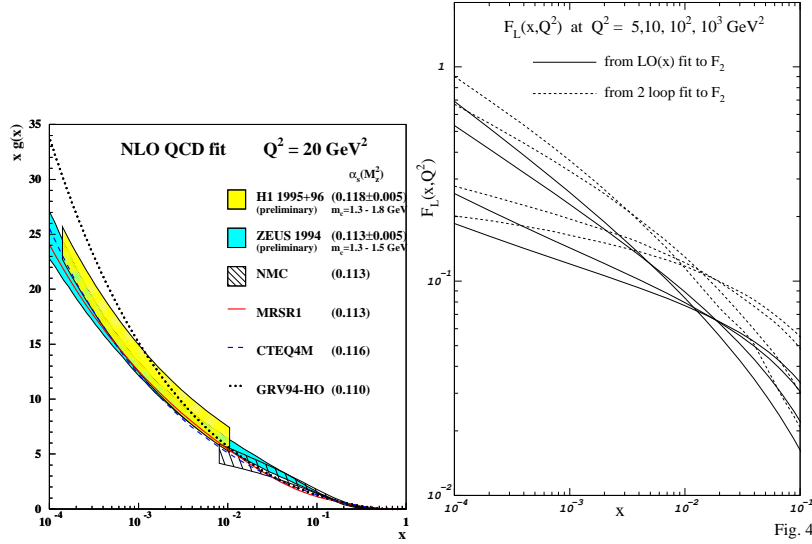


Fig. 5. Left: the gluon momentum density from H1 and ZEUS, together with an earlier result from NMC. The error bands are from the experimental systematic errors. The curves are from some recent global fits. Right: predictions for F_L at four values of Q^2 from Thorne showing the result of a standard two-loop QCD calculation and his LORSC procedure (labelled $LO(x)$).

the lower value of α_S used, but it is also known that the very low starting scale of 0.3 GeV^2 makes the gluon distribution rise too steeply at moderate Q^2 values.

Despite the manifest success of DGLAP evolution in describing F_2 data, the argument about low x QCD continues. If DGLAP is the full story then why are the large $\ln(1/x)$ terms suppressed? A number of authors [38] have investigated the need for including the $\ln(1/x)$ terms ('resummation') but come to different conclusions. The most complete approach is that of Kwiecinski, Martin and Stasto [39] which combines the BFKL and DGLAP equations and gives a reasonable representation of the low x data. Another approach to BFKL which is quite successful phenomenologically is that of the colour dipole [40]. Apart from the resummation of the leading twist log terms, it has been argued recently that higher twist (power corrections in Q^2) may be significant at low x [41] and that shadowing corrections may be larger than BFKL effects in the kinematic region of HERA data [42]. It may be that some of differences in outcome can be traced to different renormalisation schemes. A way to avoid such difficulties is to formulate the problem in terms of *physical* quantities, such as F_2 and F_L , rather than parton densities. This approach has been advocated by Catani [43] and taken furthest by Thorne [44] in his

Leading Order Renormalisation Scheme Consistent (LORSC) framework. Although only at leading order he gets slightly better fits to the low x data than the conventional DGLAP global fits. What is crucially needed to sort out these various ideas are measurements of another observable as the different schemes can all fit F_2 but then differ for the other. This is demonstrated in Fig. 5(right) for F_L .

2.3 F_L and F_2^c

All fixed target experiments, except E665, have provided measurements of F_L . The measurement requires collecting data at high y for at least two centre-of-mass energies. The most recent measurements are from SLAC/E140X [45], NMC [5, 46] and CCFR [47]. At the smallest x value of these data, $4 \cdot 10^{-3}$ from NMC, F_L is possibly rising, but the errors are rather large. The x range and precision of the F_L data are both insufficient for them to discriminate between low x models. To date HERA has run essentially at a fixed centre-of-mass energy of 300 GeV thus precluding a direct measurement of F_L . In the

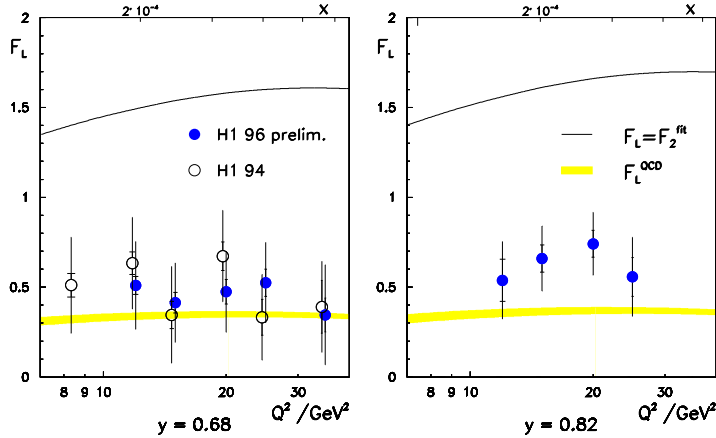


Fig. 6. Estimate of F_L by H1 from their NLO QCD fitting procedure as explained in the text.

meantime H1 has used NLO QCD and their high statistics data to make an estimate of F_L [48]. The essence of the idea is to determine F_2 for $y < 0.35$ (where the contribution of F_L to the cross-section is negligible) by a NLO QCD fit. The fit is then extrapolated to larger y and used to subtract F_2

from the measured cross-section. At this conference the results for F_L were updated by preliminary data from the HERA 1996 run [11], giving F_L at $y = 0.68$ and 0.82 , the results are shown in Fig. 6. The extrapolation is the most uncertain part of the analysis. H1 has checked that using other models for the extrapolation gives the same value for F_L to within a few percent, but it has been argued that the error could be larger [49]. The H1 estimate for F_L is compatible with pQCD calculations using recent global PDFs.

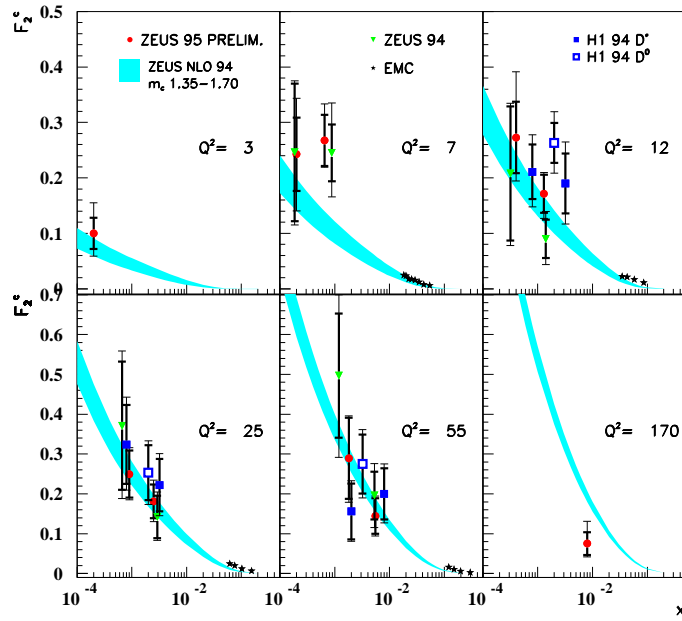


Fig. 7. Recent results from HERA on F_L^c . Earlier data from EMC is also shown. The curve shows the result of a NLO calculation allowing variation of the charm mass in the range $1.35 - 1.7$ GeV.

The calculation of the NLO coefficient functions for massive quarks by Laenen et al [50] gave an impetus for the question of how massive quarks should be included in NLO global fits. The GRV(94) fit and the fits by H1 and ZEUS include charm only by the boson-gluon fusion (BGF) process. It has been argued that this cannot be correct well above threshold when the

charm mass becomes negligible, charm should then be treated as any other light quark. This interesting subject will not be pursued here as it can be followed in refs [51], rather the status of measurements of F_2^c will be reviewed briefly. At HERA charm can contribute up to 30% of the cross-section, so it is important to understand both how to describe it theoretically and to measure it directly. The methods used by H1 and ZEUS to tag charm are by D^* , D^0 two body decays and by the $D^* - D^0$ mass difference. Statistics are limited by the small combined $D^* \rightarrow K\pi\pi$ branching ratio of only 2.6%. A major source of systematic error is the extrapolation of the measured D^* production cross-section to the full phase space in rapidity and p_T . All these matters are covered in more detail by Prinias [37]. The HERA results for F_2^c are shown in Fig. 7 together with a NLO calculation from Harris and Smith [53]. The band shows the uncertainty in the calculation, gluon densities were taken from GRV(94) or CTEQ4F but the largest source of uncertainty comes from the mass of the charm quark. The results are encouraging and their precision

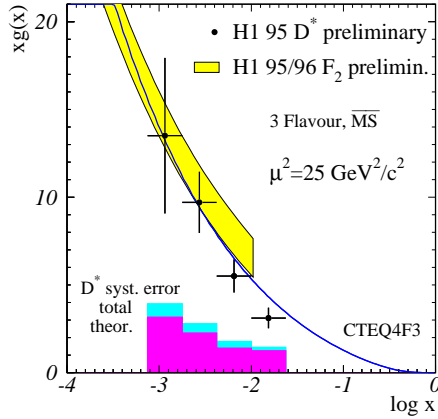


Fig. 8. Extraction of the gluon density from their 1995 D^* data together with the gluon density from scaling violations in F_2 .

will improve through higher luminosity and the use of microvertex detectors (installed in H1, planned for ZEUS). In another contribution [52], also covered by Prinias, H1 have used tagged DIS charm events from HERA(95) data to make a direct determination of the gluon density at four x values between

$0.7 \cdot 10^{-3}$ and $0.5 \cdot 10^{-1}$. The results are shown in Fig. 8 together with the gluon density determined by H1 from scaling violations in their 1995/6 F_2 data.

The material in section 2 is covered in greater detail in a recent review by Cooper-Sarkar, Devenish and De Roeck [54].

3 Nucleon Spin Structure

The challenge of polarised DIS is to understand the dynamical distribution of spin amongst the nucleon's constituents, summarised by the relation $\frac{1}{2} = \frac{1}{2}\Delta\Sigma + \Delta g + \langle L_z \rangle$ where $\Delta\Sigma$, Δg are the contributions of the quarks and gluons respectively and $\langle L_z \rangle$ is the contribution from parton orbital angular momentum. The primary measurements are the spin asymmetries for nucleon spin parallel and perpendicular to the longitudinally polarised lepton spin. They are related to the polarised structure functions g_1 , g_2 by kinematic factors. Only g_1 has a simple interpretation in terms of polarised PDFs, namely

$$g_1(x) = \frac{1}{2} \sum_f e_f^2 (q_f^\uparrow(x) - q_f^\downarrow(x)) = \frac{1}{2} \sum_f e_f^2 \Delta q_f(x) \quad (4)$$

where the sum is over quark and antiquarks with flavour f and q_f^\uparrow , q_f^\downarrow are the quark distribution functions with spins parallel and antiparallel to the nucleon spin. Full details of the formalism and QCD evolution equations may be found in ref. [55]. The observed asymmetries are reduced by the beam and target polarisations and the target dilution factor. Polarisations are usually greater than 50%, but the dilution factor is generally quite small for solid or liquid targets, typically 0.13 for butanol and 0.3 for ^3He . The HERMES

Table 2. Summary of recent polarised structure function experiments.

Lab	Beam	Targets	Experiment	x	Status
SLAC	e 29(GeV)	^3He , NH_3 , ND_3	E142/3	0.03 – 0.8	complete
SLAC	e 48	^3He , NH_3 , LiD	E154/5	0.014 – 0.7	analysis
CERN	μ 190	D- H- butanol, NH_3	SMC	0.003 – 0.7	complete
DESY	e 27	H, ^3He	HERMES	0.023 – 0.6	running

experiment at DESY uses a polarised internal gas jet target in the HERA-e beam and thus achieves a dilution factor of 1. Apart from HERMES, the latest round of experiments from SLAC and CERN is almost complete, details are given in Table 2. From the table it can be seen that the measurements of

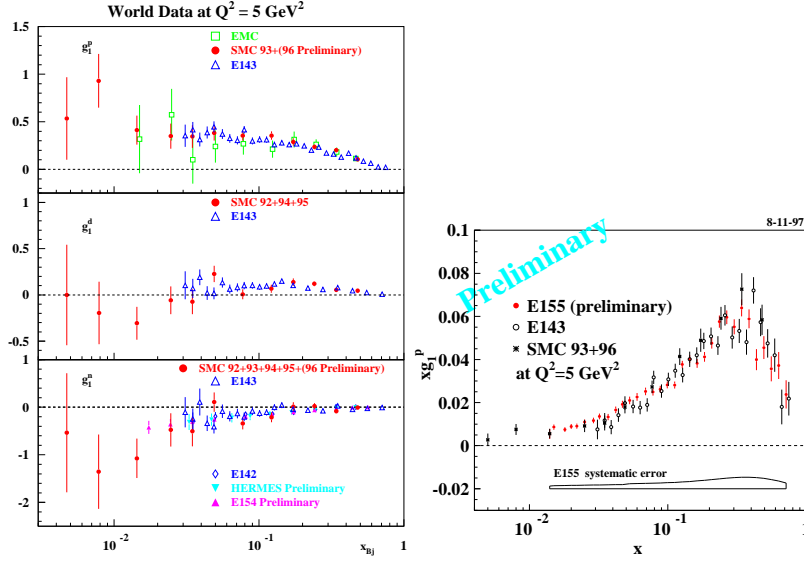


Fig. 9. Left: a compilation by the SMC collaboration of data on g_1 for protons, neutrons and deuterons from SMC, SLAC and HERMES polarised DIS experiments. Right: Preliminary data for xg_1^p from the SLAC E155 polarised DIS experiment, compared to earlier data.

polarised DIS do not reach very small values of x , the largest range is that of the SMC experiment.

Most of the data is for g_1 and there is nice agreement between the different experiments as can be seen from Fig. 9(left). There is a small amount of data for g_2 from the SLAC experiments, g_2 is small and consistent both with zero and the expectation of the twist-2 calculation. More details on the individual experiments are to be found in the contributions of Souder [56] (E154/5), Le Goff [57] (SMC) and Blouw [58] (HERMES). New preliminary data on the proton asymmetry comes from the HERMES collaboration [58] and the SLAC E155 experiment [59], both offer the prospect of reduced statistical errors as can be seen for E155 from Fig. 9(right).

Apart from more accurate data, the big advance this year has been the extensive use of NLO QCD fitting. Apart from the intrinsic interest in testing QCD, the NLO fit also gives the best extrapolation of the data to a common Q^2 for the evaluation of sum rule integrals $\Gamma_1^i(Q^2) = \int_0^1 g_1^i(x, Q^2) dx$ and the evaluation of separate parton components. The first NLO fits were performed in 1995/6 [60], this year the experimental groups SLAC/E154 [56] and SMC [57] and the theoretical teams of Altarelli et al (ABFR) [61] and Leader et al (LSS) [62] have published such analyses. There are considerable

differences of detail in the approaches taken by the different groups, perhaps the most important is the choice of factorisation scheme, LSS use $\overline{\text{MS}}$ and all other groups follow the Adler-Bardeen scheme to give a scale independent first moment for $\Delta\Sigma$, $\Delta\Sigma_{AB} = \Delta q_0 + n_f \frac{\alpha_S}{2\pi} \Delta g$. All groups assume a non-singular x dependence for the input distributions at Q_0^2 and the partonic constraint $|\Delta q_{NS}| < q_{NS}$, where NS refers to the non-singlet contribution. The quality of the fits is good and one finds that the non-singlet valence quark distributions are quite well determined. The results for the quark singlet and gluon distributions are less good as there are no data for $x < 3 \cdot 10^{-3}$. These features are shown in Fig. 10 from the ABFR fits, the two left hand plots show the quality of the fit to data (fit B) and the two right plots show $\Delta\Sigma$ (upper) and Δg (lower) for a variety of different assumptions about the low x behaviour (see [61] for details).

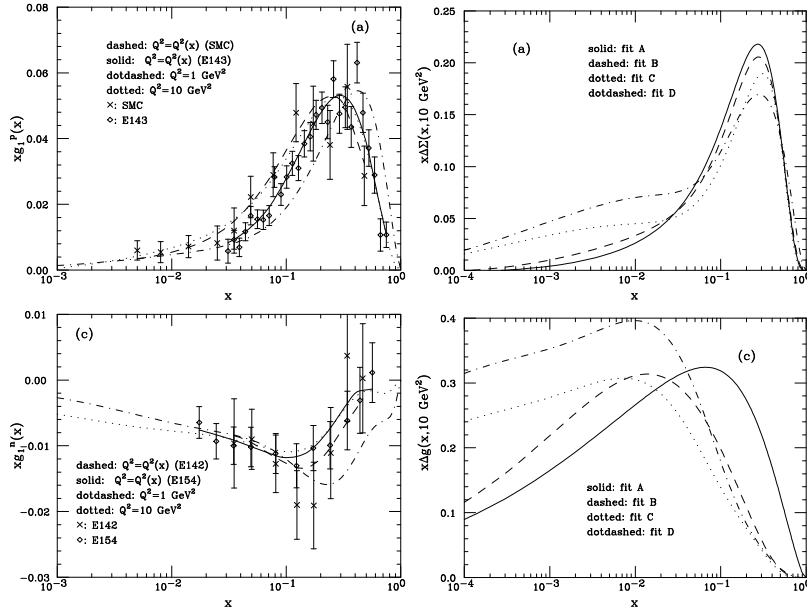


Fig. 10. From the ABFR NLO QCD fit to polarised DIS data. Left (a) xg_1^p , (c) xg_1^n ; right (a) $x\Delta\Sigma$, (c) $x\Delta g$. Curves A, B, C, D refer to fits with different assumptions for low x behaviour.

In addition to extrapolation in Q^2 , to evaluate F_1^i the data must also be extrapolated in x . There is no problem as $x \rightarrow 1$, but there is still considerable uncertainty as $x \rightarrow 0$. This is of course a reflection of both the lack of data and the range of possible behaviours for the singlet distributions at small x .

SMC has investigated this point in some detail [57] for the evaluation of Γ_1^p . Generally Γ_1^p is measured to about 10% and Γ_1^n to about 20%. For the parton components, the quark integral is known to about 10% but the gluon integral only to 40% (ABFR) and more like 100% error from the experimenters fits. All agree that the gluon contribution is positive.

What does this mean for the sum rules? The fundamental Bjorken sum rule $\Gamma_1^p - \Gamma_1^n = \frac{C_1^{NS}(Q^2)}{6} \left| \frac{g_A}{g_V} \right|$, where C_1^{NS} is a QCD coefficient known to order α_S^3 , is found to be reasonably well satisfied, at about the 10% level, by all groups. The theoretically less well found Ellis-Jaffe sum rules for Γ_1^p , Γ_1^n separately are violated at the 2σ level. The overall situation is summarised in Fig. 11.

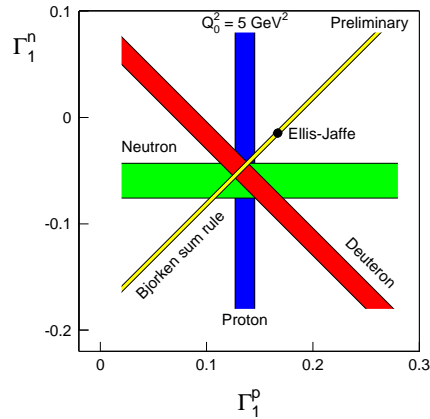


Fig. 11. Summary of the status of experimental determination of the integrals Γ_1^p , Γ_1^d , Γ_1^n and the Bjorken and Ellis-Jaffe sum rules by the SMC collaboration.

For inclusive measurements, this situation will not improve until there is data at smaller values of x , from RHIC or a polarised HERA collider. Another way to learn about individual parton distributions is through the measurement of semi-inclusive asymmetries. This type of measurement has been pioneered by the SMC whose latest results are reported by Baum [63]. HERMES has also presented some preliminary semi-inclusive results to this conference [58]. Asymmetries for identified particles such as positive or negative hadrons have been measured and from these the valence contributions Δu_V , Δd_V and the sea quark $\Delta \bar{q}$ (with some additional assumptions) deter-

mined. In the future such techniques applied to charmed particles will help to pin down the gluon contribution as well.

4 F_2^γ

The photon structure functions both for the two-lepton final states and the hadronic final state, F_2^γ , have been measured from two-photon interactions at LEP. The details of the measurements by ALEPH, DELPHI and OPAL are covered in the mini-review talk by Nisius [64]. In such measurements, only one scattered e^\pm is detected (to give the Q^2 of the event), the other giving the ‘target’ photon is lost down the beam pipe. Q^2 is measured almost directly from the tagged lepton, but x has to be deduced from the measured final state particles. The Monte Carlo modelling of the physics and detectors is thus very important and some significant improvements have been made in these areas recently [65]. The increase of the beam energies in LEP2 operations has increased both the phase space and the statistics for two-photon physics.

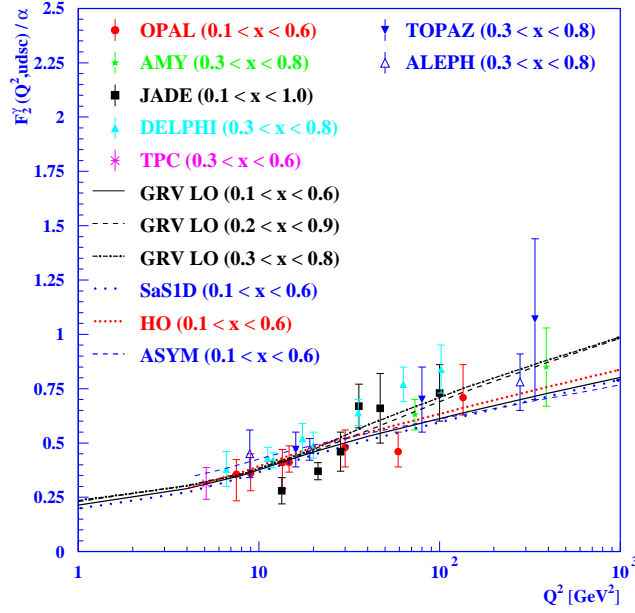


Fig. 12. Summary plot showing F_2^γ at medium x as a function of Q^2 compared to various LO and NLO QCD calculations as labelled.

Apart from the interest in determining the partonic content of the photon, the QCD evolution equations involve an inhomogeneous term which can be calculated from $\gamma \rightarrow q\bar{q}$ splitting. The data for F_2^γ are well described by NLO QCD fits and the larger lever arm in Q^2 allows one to see for the first time the logarithmic increase of F_2^γ with Q^2 , as demonstrated in Fig. 12. Because of the limited reach in small x at LEP, it has not been possible to determine if F_2^γ rises steeply as x decreases. For the same reason the gluon component of the NLO fits is not well determined.

Photoproduction processes at HERA also give information on photon structure. The process $\gamma p \rightarrow j_1 j_2 X$ is particularly attractive as it is sensitive to both direct and resolved photon processes and the kinematic variables x_γ and p_t^2 (equivalent to Q^2) can be reconstructed from the final state jets. H1 have used such a measurement to extract an effective photon PDF $\overline{f}_\gamma = f_{q/\gamma} + \frac{9}{4}f_{g/\gamma}$ for $0.2 < x_\gamma < 0.7$, the results are shown in Fig. 13. More details are given in the talk by Muller [66].

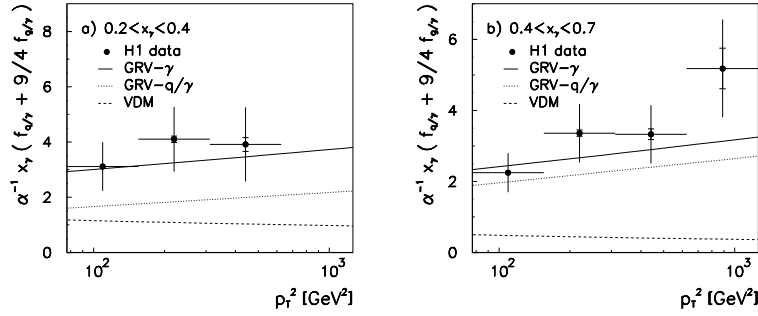


Fig. 13. The effective photon parton density \overline{f}_γ extracted from H1 1994 dijet data. The curves were calculated using GRV-LO partons and are the complete calculation (full curve), the quark component only (dotted) and the vector meson part (dashed).

Finally a more phenomenological approach to the problem of the small x region is described by Gurvich [67] in which F_2^p data at low x is used with Gribov factorisation to generate low x F_2^γ ‘data’. The generated and directly measured F_2^γ data are then fit using leading order QCD evolution over the range $4.3 < Q^2 < 390 \text{ GeV}^2$.

5 Summary and Outlook

Generally the measurements of structure functions are in good shape and the data are well described by NLO QCD. For F_2 at low x more work is needed to understand fully the implications for QCD and accurate data for an other observable such as F_L or F_2^c are essential. The understanding of both polarised structure functions and F_2^γ at small x is hampered by lack of data. Information on the nucleon gluon density is being provided by the use of charm tagging and this will improve.

For the future we can look forward to the completion of the two-photon programme at LEP2 and the large increase in luminosity promised by the HERA upgrade. The COMPASS experiment at CERN, polarised scattering at RHIC and maybe a fully polarised HERA hold out the promise of finally unravelling the mysteries of nucleon spin.

The measurement and analysis of DIS and structure functions are still challenging our understanding of hadronic structure and QCD 30 years after the discovery of scaling.

Acknowledgements

I thank my colleagues in H1 and ZEUS for providing information and insights on the latest HERA results. I thank A. Brüll, J. Le Goff and E. Rondio for instructions on spin physics, likewise D. Miller, R. Nisius and S. Söldner-Rembold on two-photon physics. I thank the organisers of the Conference, particularly D. Lellouch, and IT staff at Oxford and Jerusalem for much practical help.

References

- [1] H. Weerts, Plenary talk PL1, these proceedings.
- [2] R. Eichler, Plenary talk PL2, these proceedings, [hep-ex/9712011](#).
- [3] D. Ward, Plenary talk PL15, these proceedings, [hep-ph/9711515](#).
- [4] E. Elsen, Plenary talk PL26, these proceedings.
- [5] NMC, M. Arneodo et al, Nucl. Phys. B483 (1997), 3.
- [6] E665, M. R. Adams et al, Phys. Rev. D54 (1997), 3006
- [7] H1, S. Aid et al, Nucl. Phys. B470 (1996), 3.
- [8] ZEUS, M. Derrick et al, Z. Phys. C72 (1996), 399.
- [9] CCFR, W. G. Seligman et al, Phys. Rev. Lett. 79 (1997) 1213.
- [10] L. De Barbaro, Invited talk 316, these proceedings.
- [11] H1, Submitted paper 260 to this conference.
- [12] U. Bassler, Invited talk 31302, these proceedings.
- [13] H1, C. Adloff et al, Nucl. Phys. B497 (1997) 3.
- [14] ZEUS, J. Breitweg et al, Phys. Lett. B407 (1997) 43.
- [15] ZEUS, Submitted paper 646 to this conference.
- [16] M. Glück, E. Reya & A. Vogt, Z. Phys. C48 (1990) 471; C53 (1992) 127.

- [17] M. Glück, E. Reya & A. Vogt, *Z. Phys.* C67 (1995) 433.
- [18] A. Donnachie & P. V. Landshoff, *Phys. Lett.* B296 (1992) 227; *Z. Phys.* C61 (1994) 139.
- [19] ZEUS, Submitted paper 647 to this conference.
- [20] A. Capella et al, *Phys. Lett.* B337 (1994) 358.
- [21] H. Abramowicz et al, *Phys. Lett.* B269 (1991) 465.
- [22] B. Badelek & J. Kwiecinski, *Phys. Lett.* B295 (1992) 263.
- [23] D. Schildknecht & H. Spiesberger, preprint BI-TP-97-25
- [24] G. Kerley & G. Shaw, preprint MC-TH-97-12
- [25] E. Gotsman, E. M. Levin & U. Maor, [hep-ph/9708275](#).
- [26] K. Adel, F. Barreiro & F. J. Yndurain, *Nucl. Phys.* B495 (1997) 221.
- [27] V. Shekelyan, invited talk at the 1997 International Symposium on Lepton and Photon Interactions, Hamburg July 1997.
- [28] H. Abramowicz & A. Levy, DESY 97-251 [hep-ph/9712415](#).
- [29] B. Badelek & J. Kwiecinski, *Rev. Mod. Phys.* 68 (1996) 445.
- [30] E. A. Kuraev, L. N. Lipatov & V. Fadin, *Soviet Phys. JETP* 45 (1977) 199; Ya. Balitsky & L. N. Lipatov, *Soviet J. Nucl. Phys.* 28 (1978) 822.
- [31] F. Eisele, Proc. of EPS HEP95 Conference Brussels Aug. 1995 eds J. Lemonne, C. Vander Velde & F. Verbeure, World Scientific p709.
- [32] R. D. Ball & S. Forte, *Phys. Lett.* B335 (1994) 77; *Phys. Lett.* B336 (1994) 77; *Acta Physica Polonica* B26 (1995) 2097.
- [33] CTEQ4, H. Lai et al, *Phys. Rev.* D55 (1997) 1280.
- [34] MRS(R), A. D. Martin, R. G. Roberts & W. J. Stirling, *Phys. Lett.* B387 (1996) 419.
- [35] S. Bethke, *Nucl. Phys. Proc. Supp.* 54A (1997) 314.
- [36] M. Virchaux & A. Milsztajn, *Phys. Lett.* B274 (1992) 221.
- [37] A. Prinias, Invited talk 315, these proceedings.
- [38] For example: J. Blümlein & A. Vogt, submitted paper 751 to this conference; J. R. Forshaw et al, *Phys. Lett.* B356 (1995) 79; I. Bojak & M. Ernst, *Phys. Lett.* B397 (1997) 296.
- [39] J. Kwiecinski, A. D. Martin & A. M. Stasto, *Phys. Rev.* D56 (1997) 3991.
- [40] C. Royon, Invited talk 313, these proceedings.
- [41] J. Bartels & C. Bontus, Proc. DIS97 Chicago, <http://www.hep.anl.gov/dis97/>.
- [42] E. M. Levin, Invited talk at the Conference on Perspectives in Hadronic Physics Trieste May 1997 [hep-ph/9706448](#); M. Gay Ducati, Invited talk 318, these proceedings
- [43] S. Catani, *Z. Phys.* C75 (1997) 665.
- [44] R. S. Thorne, *Phys. Lett.* B392 (1997) 463; [hep-ph/9710541](#).
- [45] L. H. Tao et al, *Z. Phys.* C70 (1996) 387.
- [46] A. J. Milsztajn, Proc. DIS96 Rome Eds G. D'Agostini & A. Nigro, World Scientific 1997 p213.
- [47] U. K. Yang, *J. Phys.* G22 (1996) 775.

- [48] H1, C. Adloff et al, Phys. Lett. B393 (1997) 452.
- [49] R. S. Thorne, [hep-ph/9708302](#).
- [50] E.Laenen et al, Nucl. Phys. B291 (1992) 325; B392 (1993) 162,229; S. Riemersma et al, Phys. Lett. B347 (1995) 143.
- [51] See the discussion at DIS97 Chicago and H. L. Lai & W. K. Tung, Z. Phys. C74 (1997) 463; A. D. Martin et al [hep-ph/9612449](#); M. Buza et al [hep-ph/9612398](#); R. G. Roberts & R. S. Thorne [hep-ph/9711213](#).
- [52] H1, submitted paper 275 to this conference.
- [53] B. W. Harris & J. Smith, [hep-ph/9706334](#).
- [54] A. M. Cooper-Sarkar, R. Devenish & A. De Roeck, [hep-ph/9712301](#), to be published in IJMPA.
- [55] M. Anselmino, A. Efremov & E. Leader, Phys. Rep. 261 (1995) 1, erratum 281 (1997) 399.
- [56] E154/4, P. Souder, Invited talk 301, these proceedings; K. Abe et al, Phys. Rev. Lett. 79 (1997) 26.
- [57] SMC, J. Le Goff, Invited talk 303, these proceedings; D. Adams et al, Phys. Rev. D56 (1997) 5330.
- [58] HERMES, J. Blouw, Invited talk 302, these proceedings.
- [59] E155, S. E. Rock, private communication.
- [60] M. Glück et al, Phys. Rev. D53 (1996) 4775; T. Gehrmann & W. J. Stirling, Phys. Rev. D53 (1996) 6100.
- [61] G. Altarelli et al, Nucl. Phys. B496 (1997) 337.
- [62] E. Leader, A. V. Sidorov & D. B. Stamenov, [tt hep-ph/9708335](#).
- [63] SMC, G. Baum, Invited talk 304, these proceedings.
- [64] R. Nisius, Invited talk 306, these proceedings, [hep-ex/9712012](#).
- [65] D. Miller, Summary talk at Photon97 Amsterdam May 1997, [hep-ex/9708002](#).
- [66] H1, K. Muller, Invited talk 307, these proceedings.
- [67] E. Gurvich, Invited talk 308, these proceedings.